Research Article

Tao Meng*, Kanjun Ying, Xiufen Yang, and Yongpeng Hong

Comparative study on mechanisms for improving mechanical properties and microstructure of cement paste modified by different types of nanomaterials

https://doi.org/10.1515/ntrev-2021-0027
received April 9, 2021; accepted May 6, 2021

Abstract: Filling and nucleation are the mechanisms of modifying cement paste with nanomaterials, as investigated by previous studies, and are difficult to reflect the different effects of nanomaterials, especially on the changes of cement clinker and hydration products in the cement hydration process. In this study, the mechanisms of modifying cement paste with nano-calcium carbonate (NC), nano-graphene oxide (NG), nano-silica (NS), and nano-titanium dioxide (NT) were investigated by determining the mechanical properties of cement paste treated with nanomaterials and analysing the changes in the cement clinker (tricalcium silicate and dicalcium silicate), hydration products (portlandite and ettringite), and microstructure through many micro-test methods. The results indicate that the incorporation of nanomaterials could improve the early strength of cement paste specimens due to more consumption of cement clinker. Meanwhile, different nanomaterials promote the formation of different hydration products at early ages. C–A–S–H gel, flower-like ettringite, and C–S–H seeds are widely distributed in the cement paste with the incorporation of NC, NG, and NS, respectively. NT exhibits insignificant nucleation effect and has inhibitory effect on portlandite precipitation. This study provides key insights into the mechanism of nanomaterials from the perspective of cement hydration, which may promote the further research and application of nanomaterials in the cement and concrete industries.

Keywords: nanomaterials, mechanical properties, microstructure

* **Corresponding author: Tao Meng,** Institute of Engineering Materials, College of Civil Engineering and Architecture, Zhejiang University, Hangzhou 310058, China, e-mail: taomeng@zju.edu.cn
Kanjun Ying, Xiufen Yang: Institute of Engineering Materials, College of Civil Engineering and Architecture, Zhejiang University, Hangzhou 310058, China
Yongpeng Hong: Institute of Engineering Materials, College of Civil Engineering and Architecture, Zhejiang University, Hangzhou 310058, China; Contract Management Department, China Overseas Property Co., Ltd., Fuzhou 350108, China

1 Introduction

When the particle size of a material is reduced to the range of 1–100 nm, the resulting nanoparticles exhibit novel physical and chemical properties. The differences in the structure of the nanomaterials relative to that of the macromaterial are that the former have a large specific surface area, and the state of their surface atoms is closer to the gaseous state, forming neither long-range nor short-range amorphous layers, while the atoms inside the nanoparticles may be in an orderly arrangement. Owing to the small particle size and large surface curvature of nanomaterials, there is a high internal pressure, which can deform the internal structure, triggering small volume effects, surface effects, quantum size effects, and macroscopic quantum tunnelling effects [1,2]. In the last few years, an increasing number of scientists have devoted themselves to studying nanomaterials, including the application of nanomaterials to cement-based material reinforcement, and have achieved fruitful results in the preparation, property modification, and application of nanomaterials [3].

Nano-silica (NS) is the earliest and currently most widely used nanomaterial. Based on the different preparation processes, the types of NS are divided into powder, colloid, and dispersion. To strengthen cement-based materials, colloidal NS and NS dispersions are generally used to uniformly disperse NS in cement-based materials. It has been proven that NS can effectively improve the workability, strength, and durability of cement-based materials, and the reinforcing effect of NS

is better than that of silica fume because of its stronger filling effect and greater pozzolanic activity [4–16]. However, more water is consumed in the cement hydration process due to the large specific area of NS, which significantly affects the rheological properties of cement-based materials [17], and the price of NS is very high, limiting the application of NS in construction engineering.

Relatively cheap nano-calcium carbonate (NC) and nano-titanium dioxide (NT) have drawn widespread attention. Studies have shown that the hydration reaction of NC with C_3A in cement clinker changes the early hydration products, and the microhardness and elastic modulus of the early hydration products are significantly improved [18]. At the same time, NC also has a filling effect and can act as a nucleation site to accelerate the hydration process, thereby significantly improving the early strength of cement-based materials [19–24]. Moreover, NC has little effect on the water required by cement-based materials to achieve standard consistency. However, excessive addition of NC seriously affects the workability and drastically reduces the later strength of cement-based materials [25]. Because NT has the ability to block ultraviolet rays, as well as induce sterilisation and the photolysis of organic pollutants, it has attracted significant research interest. When applied to cement-based materials, NT can provide additional photocatalysis and self-cleaning functions, but the incorporation of NT will cause adverse effects on the strength and fluidity of cement-based materials [26,27].

With the advancement of graphene application technology, nano-graphene oxide (NG), which has excellent performance, has begun to be used for reinforcing cement-based materials. NG can be regarded as a nucleation site for accelerating the hydration process and is likely to unite hydration products to form a dense microstructure [28–30]. Oxygen-containing groups (such as carboxyl, hydroxyl, and carbonyl) in NG can be dispersed in the micropores of cement-based materials [31–35]; these groups play a role in modifying the microstructure of the cement matrix and further promoting cement hydration. In addition, the two-dimensional structure of graphene oxide itself can provide a template for cement hydration [29–31].

Most studies have shown that the incorporation of nanomaterials significantly increases the early strength of cement-based materials but reduces their later strength. However, some researchers reported that the addition of 4% nano-silica improved the compressive strength of cement paste to 95.3 MPa at 28 days, which is 13% higher than that of the blank control group [36]. The results of previous studies are difficult to match and are even contradictory; thus, it is difficult to draw statistically verified conclusions. Moreover, the incorporation of nanomaterials could promote the formation of early hydration products, such as $Ca(OH)_2$ and C–S–H gel, but quantitative analysis of hydration products has seldom been undertaken. The mechanism by which nanomaterials modify the properties of cement-based materials is still unclear, and different types of nanomaterials with different characteristics must exhibit significant differences in terms of technical performance. Therefore, it is necessary to study the effects of different types of nanomaterials on the mechanical properties and microstructure of cement paste to provide a basis for deeper understanding of the mechanism by which nanomaterials modify cement paste.

In this study, four different types of nanomaterials (NC, NG, NS, and NT) are explored to study the mechanical properties and microstructure of cement paste, particularly at 1 and 28 days. As shown in graphical abstract, thermogravimetric-differential thermal analysis (TG–DTA), quantitative X-ray diffraction (XRD) analysis, Fourier-transform infrared (FTIR) spectrometry, mercury intrusion porosimetry (MIP), and scanning electron microscopy (SEM) are used to reveal the mechanisms of action of the different types of nanomaterials. This study finally proposes the hydration models and hydration reactions of cement to provide key insights into the effects of different types of nanomaterials on the properties and microstructure of cement-based materials.

2 Materials and methods

2.1 Materials

P.O. 42.5 cement according to Chinese standard GB 175-2007 and tap water were used for the test. The four most concerned nanomaterials were selected for experimental research. XFI24 colloid NS (particle size: 20–30 nm; solid content: 30 wt%), XFI22 colloid NT (particle size: 10–20 nm; solid content: 20 wt%), and XF020 NG dispersion (diameter: 50–200 nm; single layer ratio: ~99%; thickness: 0.8–1.2 nm; purity: ~99%; solid content: 0.1 wt%) produced by Nanjing/Jiangsu XFNANO Materials Tech Co., Ltd. The NC slurry with 3% solid content was developed independently at the Institute of Engineering Materials, Zhejiang University. The colloid NS, colloid NT, and NG dispersion were uniformly dispersed with an ultrasonic disperser to avoid agglomeration. Meanwhile, constant temperature magnetic stirring equipment was used for effective dispersion of the NC slurry. The NC slurry was used immediately after preparation, which could effectively avoid agglomeration. As the cost of nanomaterials continues to decrease, it is of great significance for the application of nanomaterials in practical engineering.

2.2 Preparation of cement paste

Keep the water–binder (binder: cement and nanomaterials) ratio of cement paste at 0.35, the proportions of components in the mix for the cement paste specimens are listed in Table 1. The cement was mixed slowly in a mixer for 120 s, allowed to stand for 15 s, and then mixed quickly for 120 s. The cement paste was then poured into six-joint copper moulds with dimensions of 20 mm × 20 mm × 20 mm and consolidated using a vibration table. The specimens were maintained at a constant temperature of 20°C for 24 h. After demoulding, the specimens were kept under standard curing conditions (temperature of 20 ± 2°C and relative humidity of 95% or greater) until the testing stage.

2.3 Compressive strength

The compressive strength of the analysed cement paste samples was measured by WDW-100 universal testing machine according to GB/T50081-2002. Uniaxial compressive loads were applied at a loading rate of 0.5 kN/s until the specimens failed. Three specimens were tested for each scenario for a specific curing age, and the averages of these three replicates were calculated.

2.4 TG–DTA

TG–DTA was performed using an SDT Q600 (TA Instruments, USA). The samples were the same as those used for XRD analysis. The samples (10 mg) were heated at a rate of 10°C/min from room temperature to 1,000°C, with gaseous N_2 flowing at a rate of 120 mL/min.

Table 1: Composition of mix for cement paste specimens (wt%)

Mix	Cement	Water	Nanomaterials (wt% of original cement)
N-0	100	35	0
NC-0.15	99.85	35	0.15
NC-0.3	99.7	35	0.3
NC-0.45	99.55	35	0.45
NC-0.6	99.4	35	0.6
NG-0.01	99.99	35	0.01
NG-0.02	99.98	35	0.02
NG-0.03	99.97	35	0.03
NG-0.04	99.96	35	0.04
NS-1.5	98.5	35	1.5
NS-3	97	35	3
NS-4.5	95.5	35	4.5
NS-6	94	35	6
NT-1	99	35	1
NT-2	98	35	2
NT-3	97	35	3
NT-4	96	35	4

2.5 XRD

For each analysed cement paste, hydration was stopped by applying pure alcohol at a specific age. Before the test, the specimens were dried in an oven at 60°C for 48 h and ground to a residue ratio on the 45 μm sieve of less than 2%. Mineralogical investigations were performed by XRD analysis, using a Bruker D8 Advance XRD instrument and a Cu-Kα X-ray radiation source. The step size was 0.02°, and the acceleration voltage was 40 kV. The 2θ scanning range was from 5° to 90°. Following the scanning, the raw diffraction data were located in the PDF-2004 database to identify peaks in the XRD pattern using MDI Jade 6.0 software, and phase quantification was conducted using Rietveld refinement analysis.

2.6 FTIR

FTIR spectra were obtained for the powdered cement paste samples, which were the same as those used for the XRD analysis, by employing a Perkin Elmer FTIR spectrometer in transmittance mode, from 400 to 4,000 cm^{-1}, using the standard KBr technique.

2.7 MIP

The prepared cement paste specimens cured for 28 days were broken into small fragments after the compressive strength test and dried in an oven at 60°C for 48 h. Thereafter, MIP tests were conducted using an AutoPore IV 9500 instrument. The mercury contact angle θ was 130.0°, and the surface tension of mercury (σ) was set to 485.0 dynes/cm in this test.

2.8 SEM

For the SEM analysis, the cement paste specimens were broken into small fragments after the compressive strength test, and hydration was stopped using pure alcohol at a specific curing age. These small fragments were sprayed with gold for 60 s to make the specimens conductive. The microscopic structures of these specimens were observed at different magnifications using a Gemini 300 SEM device.

3 Results and discussion

3.1 Compressive strength

The compressive strength of the cement paste specimens is shown in Figure 1. The results indicate that the incorporation of NS, NC, and NG could improve the early compressive strength of the cement paste specimens at 1, 3, and 7 days. For example, the compressive strength of specimen with 0.3% NC was 27.1% higher at 1 day, 20.2% higher at 3 days, and 25.8% higher at 7 days than that of N-0. However, incorporation of the nanomaterials was not conducive to improving the late compressive strength of the cement paste specimens. Surprisingly, the compressive strength of the cement paste specimens with 0.03% NG was still 10.9% higher than that of N-0 at 28 days. Incorporation of NT at low loadings of 1% and 2% can strengthen the cement paste specimens, whereas the compressive strength of the cement paste specimens exhibited a precipitous decline in both the early and late stages when the content of NT exceeded 3%. Excessive incorporation of NT will cause its uneven distribution in the cement paste, enrichment, or agglomeration in some areas, which will cause the decrease of mechanical properties.

3.2 TG–DTA

TG–DTA can identify the phase of the cement paste qualitatively and can be used to quantify the content of calcium hydroxide (CH). By monitoring the dehydration (Ldh), dihydroxylation (Ldx), and decarbonation (Ldc) of cement paste in different temperature regions, the hydration degree can also be calculated according to the method proposed by Bhatty [37].

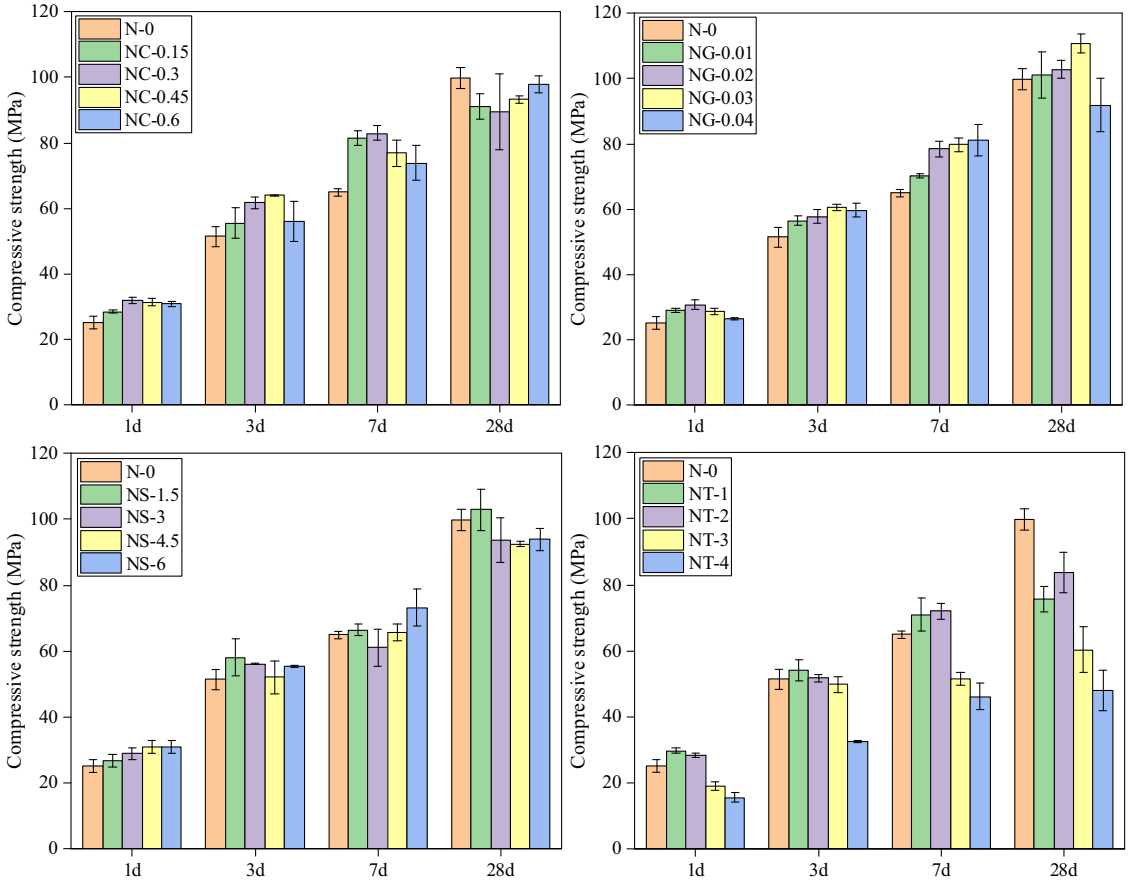

Figure 1: Compressive strength of the specimens with or without nanomaterials.

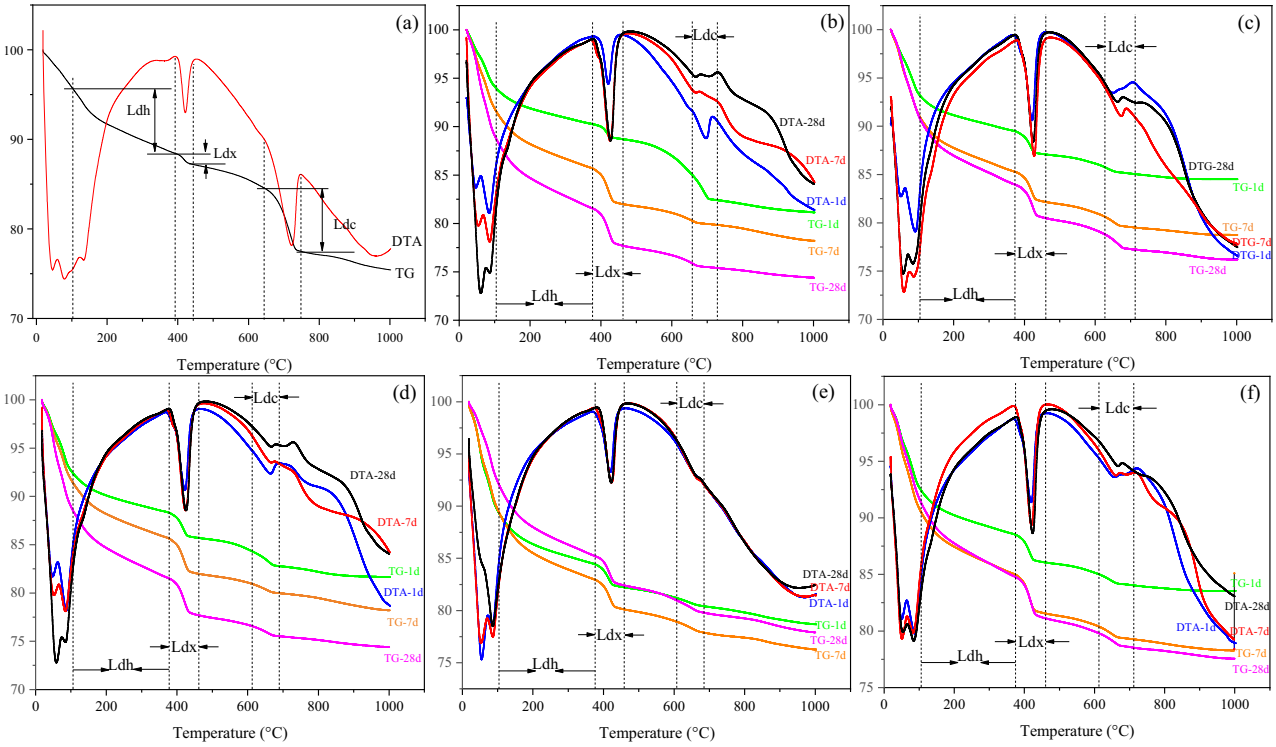

Figure 2: TG–DTA curves of the specimens. (a) Typical curves, (b) N-0, (c) NC-0.3, (d) NG-0.03, (e) NS-6, (f) NT-2.

Figure 2a serves as an example for defining the Ldh, Ldx, and Ldc temperature ranges. In this study, the temperature ranges for Ldx and Ldc were individually calculated for each sample from the derivative of the TG curve. The Ldh temperature ranges were different from those in other studies. Here, we defined the temperature range of Ldh from the beginning of heating to the start of Ldx. The TG–DTA curves of the cement paste specimens with or without nanomaterials are shown in Figure 2b–f.

The degree of hydration (α) according to Bhatty can be summarised in equations (1) and (2) [38]:

$$W_c = \text{Ldh} + \text{Ldx} + 0.41\text{Ldc}, \quad (1)$$

$$\alpha = w_c/0.24 \times 100, \quad (2)$$

where W_c is the chemically bound water, W_c, Ldh, Ldx, and Ldc are expressed in parts per unit, and α is expressed as a percentage. The definition of the parameters 0.41 and 0.24 is expounded elsewhere by Monteagudo *et al.* [39].

The hydration degree of the cement paste specimens with and without nanomaterials is shown in Figure 3. Notably, for the cement paste with incorporated nanomaterials, the hydration degree at 1 day was universally higher than that of N-0, which is consistent with the compressive strength data presented in Figure 1. Moreover, the hydration degree was greater than that of N-0 only in the case of NG-0.03 at 28 days, which determined its higher 28 days compressive strength.

3.3 Quantitative XRD analysis

The XRD patterns and the results of quantitative XRD analysis of the specimens with or without nanomaterials

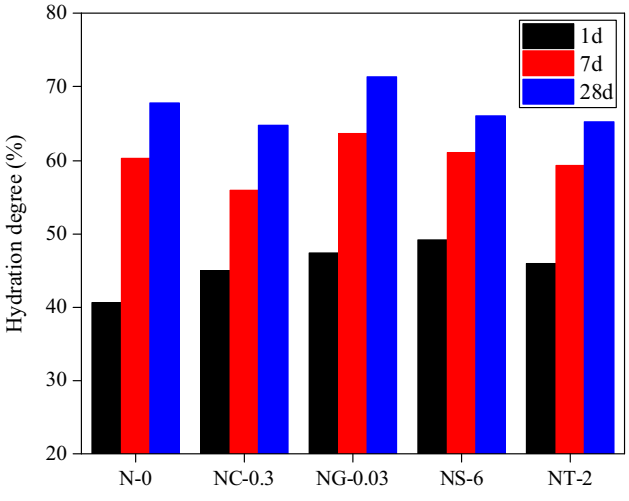

Figure 3: Hydration degree of the specimens with or without nanomaterials.

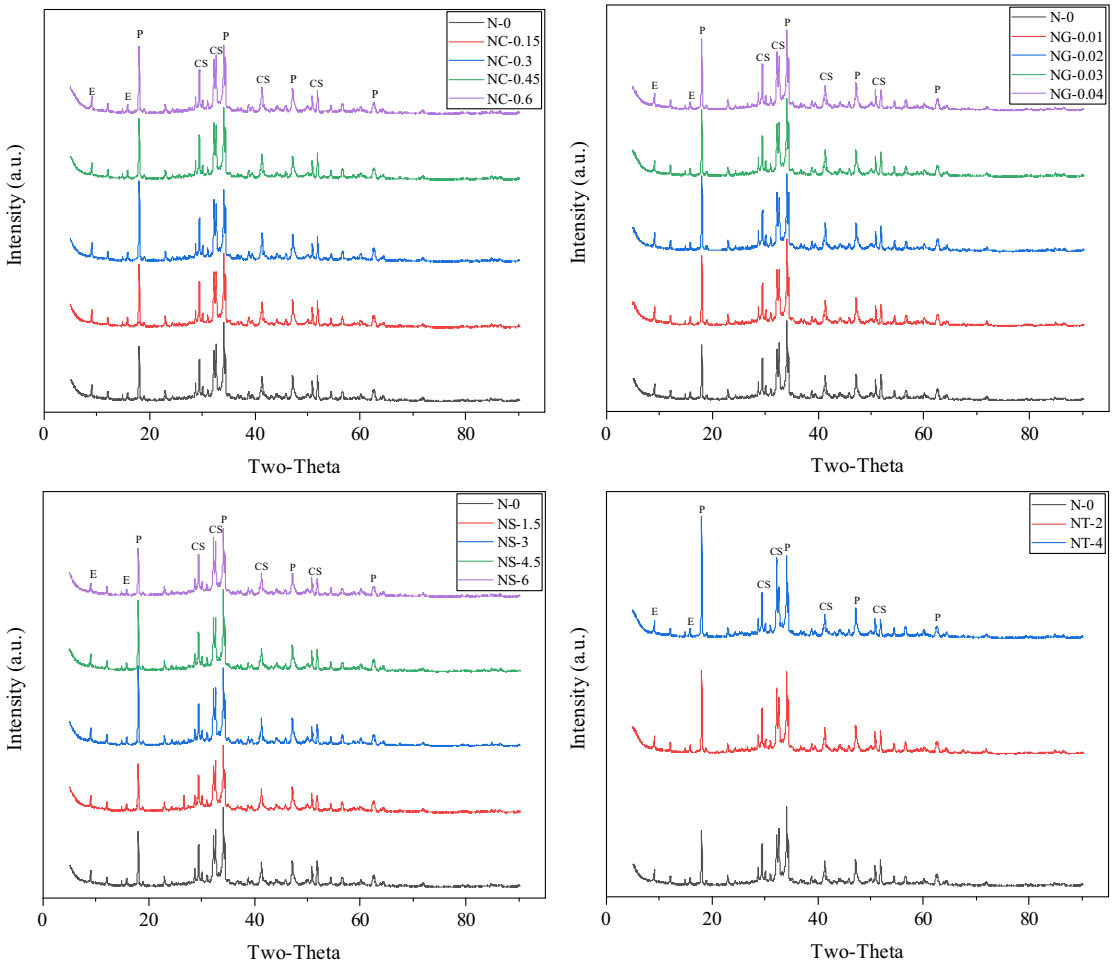

Figure 4: XRD patterns of the specimens with or without nanomaterials at 1 day (E: ettringite; P: portlandite [CH]; CS: C_3S and C_2S).

at 1 day are shown in Figures 4 and 5. Two main indicators were considered to reveal the mechanism by which the nanomaterials influence the cement-based materials. The first indicator is the consumption of cement clinker (tricalcium silicate [C_3S] and dicalcium silicate [C_2S]), and the other is the production of hydration products (ettringite and CH). With a gradual increase in the NC content, the consumption of C_3S and C_2S first increased and then decreased, reaching a maximum when the NC dosage was 0.45%. This illustrates that NC can accelerate the hydration reaction of the main clinker phases, such as C_3S and C_2S. However, the data showed that more ettringite and less CH were formed with the incorporation of 0.45% NC, which resulted in less C–S–H gel in the cement paste. Therefore, the compressive strength of the NC-0.3 cement paste specimen was higher than that of NC-0.45. This was proved by the production of CH (that could also contribute to the early strength), which reached the maximum value when the NC content was 0.3%. With a gradual increase in the NG content, the

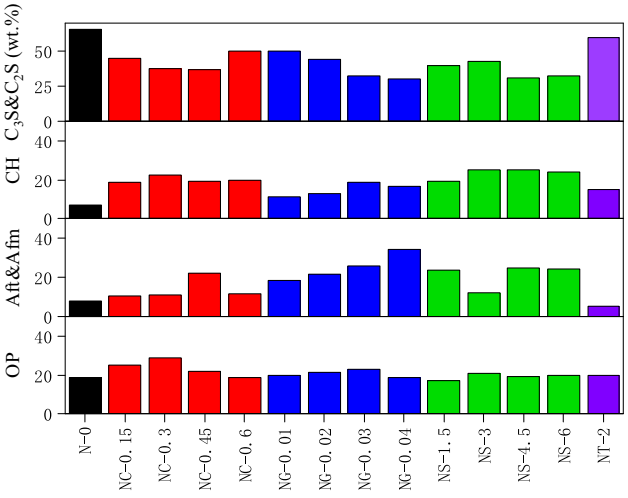

Figure 5: Results of quantitative XRD analysis of the specimens at 1 day (Aft & Afm: ettringite; OP: other phases).

consumption of C_3S and C_2S was relatively large and gradually increased, and a large amount of ettringite was formed. Therefore, the compressive strength of the cement paste specimens at 1 day was greatly improved. The C_3S and C_2S consumption was not significantly different for the cement paste with different loadings of NS, although there was a certain fluctuation, and the C_3S and C_2S consumption was also much higher than that of N-0. Note that the CH content of the NS and NT groups was also much higher than that of N-0, which may contribute to the increase in the compressive strength with the addition of these materials. However, with the addition of NT-2, the consumption of C_3S and C_2S showed little improvement compared with that of N-0, leading to a modest increase in the compressive strength of NT-2.

The XRD patterns and the results of quantitative XRD analysis of the specimens with or without nanomaterials at 28 days are shown in Figures 6 and 7. Compared with the cement paste containing nanomaterials, the consumption of C_3S and C_2S in N-0 was significantly higher (by 25.6 wt%). With the exception of NG-0.03 for which the C_3S and C_2S consumption was greater than that of N-0, for the other groups of samples, the C_3S and C_2S consumption was less than that of N-0 at 28 days, which may be the main reason for the 28 days macroscopic changes in the compressive strength of these samples. In addition, the ettringite content of NG-0.03 and NS-6 was still higher than that of N-0 at 28 days. However, ettringite contributed little to the later compressive strength of the cement paste specimens.

3.4 FTIR

The FTIR patterns of the cement paste specimens at 1 and 28 days are shown in Figure 8. The peak of the O–H stretching vibration of the hydration product (CH) appeared at 3,640 cm^{-1}, the peak of the Si–O stretching vibration of C–S–H appeared at 980 cm^{-1}, and the Si–O stretching vibration of ettringite appeared at 1,100 cm^{-1}. The types of cement hydration products formed by grinding and

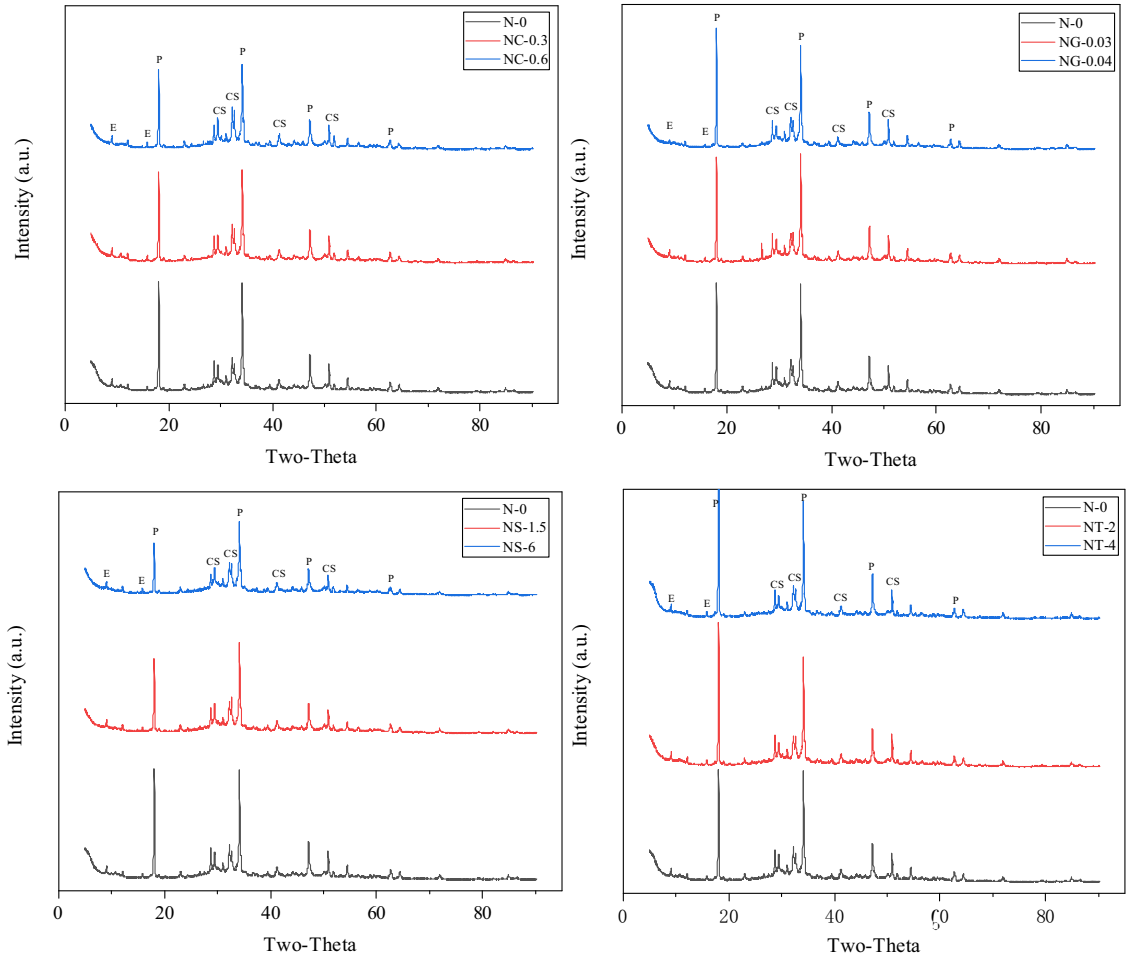

Figure 6: XRD patterns of the specimens with or without nanomaterials at 28 days (E: ettringite; P: portlandite [CH]; CS: C_3S and C_2S).

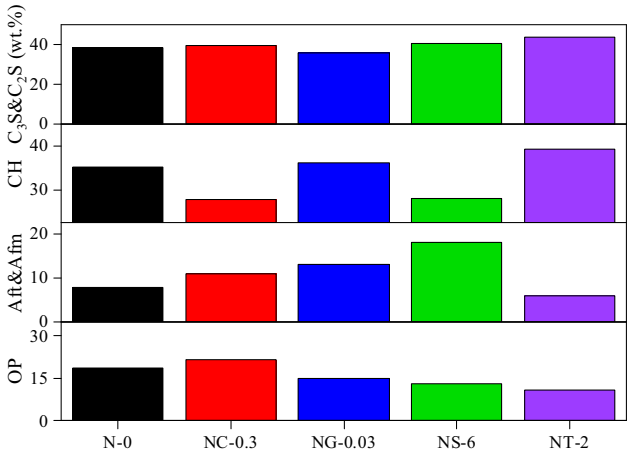

Figure 7: Results of quantitative XRD analysis of the specimens at 28 days (Aft & Afm: ettringite; OP: other phases).

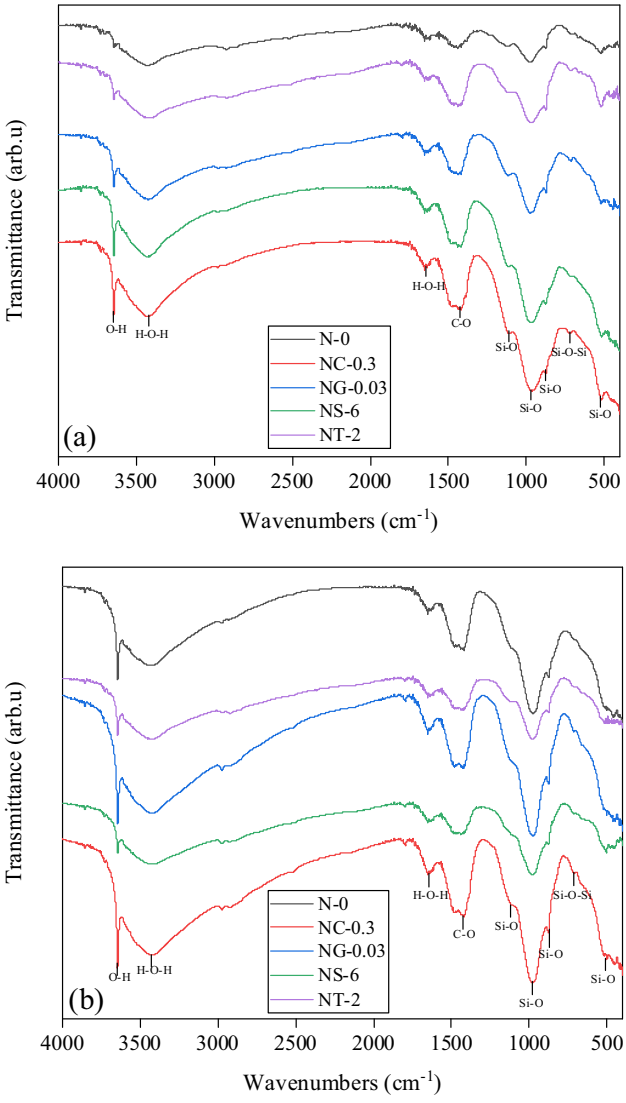

Figure 8: FTIR patterns of the specimens with or without nanomaterials at 1 and 28 days. (a) FTIR patterns of the specimens with or without nanomaterials at 1 day. (b) FTIR patterns of the specimens with or without nanomaterials at 28 days.

incorporating nanomaterials can be determined from the IR absorption profile, as shown in Figure 8a. The patterns from top to bottom show that the intensity of the O–H and Si–O peaks at 3,640 and 980 cm^{-1}, respectively, gradually increased, indicating that nanomaterials other than NT could accelerate the formation of hydration products. The O–H stretching vibration of the hydration product CH at 3,640 cm^{-1} gradually became sharper, and the symmetry of the absorption peak increased. This indicates that the nanomaterials may improve the structural arrangement of CH in the cement matrix. Comparative analysis of the FTIR patterns of the 1 and 28 day samples shows that the intensity of both peaks at 3,640 cm^{-1} (O–H) and 980 cm^{-1} (Si–O) increased to varying degrees over time. Except with the incorporation of NS, the intensity of the O–H peak decreased, indicating that NS can undergo secondary hydration with CH, thereby reducing CH. Second, the peak intensity of Si–O for the samples with NC and NT increased slightly at 28 days, which was reflected in the 28-day compressive strength of these samples compared with that of the other groups. In addition, the Si–O peak for N-0 and NG-0.03 at 28 days increased significantly, which was also reflected in the higher 28-day compressive strength compared to that of the other groups. At the same time, the symmetry of the Si–O peak at 980 cm^{-1} was significantly improved after doping with the nanomaterials, indicating that the nanomaterials could also improve the structure of the C–S–H gel.

3.5 MIP

The pore structure curves and porosity of the specimens with or without nanomaterials at 1 and 28 days are shown in Figure 9. At 1 day, the pore structure curve of the specimens with 6% NS was shifted to the left compared to that of N-0. The pore volume was larger, with pores of small diameters (0–30 nm), indicating that NS can not only refine the pore size of the cement paste but also promote the formation of nanopores, which leads to decreased porosity. In comparison, the pore structure curve of NC-0.3 was greatly skewed to the left compared to that of N-0, which shows that NC only refined the pore diameter, with a slight decrease in porosity. In contrast, the pore structure curves of NG-0.03 and NT-2 were shifted slightly to the right compared to those of N-0, which indicates that NG and NT had little effect on the

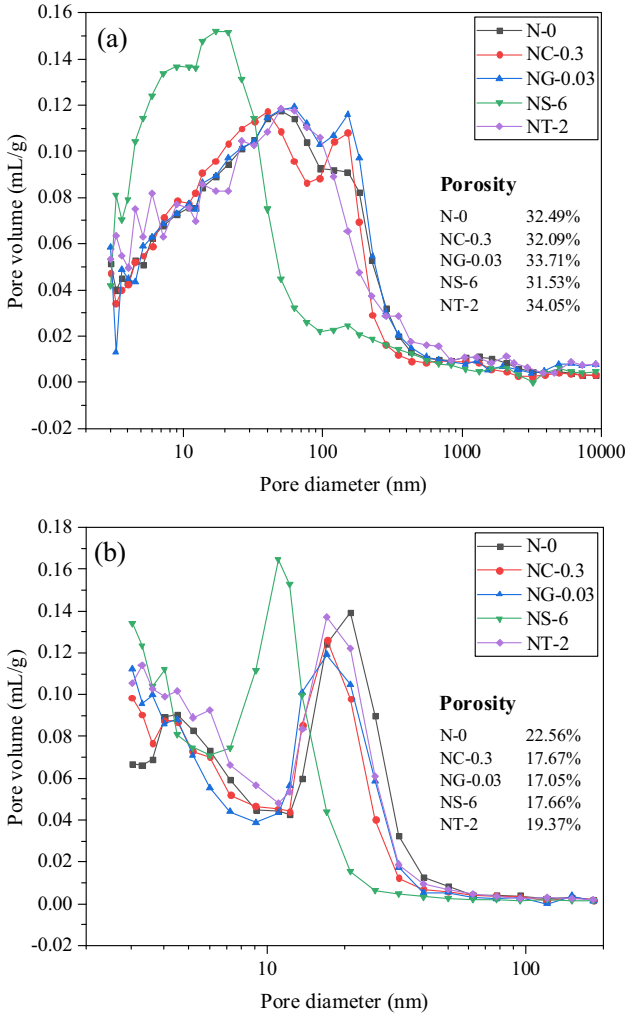

Figure 9: Pore structure curves and porosity of the specimens with or without nanomaterials at 1 and 28 days. (a) Pore structure curves and porosity of the specimens with or without nanomaterials at 1 day. (b) Pore structure curves and porosity of the specimens with or without nanomaterials at 28 days.

pore structure at 1 day. The overall pore structure curves of the specimens at 28 days, as shown in Figure 9b, were shifted to the left compared with those of the specimens at 1 day, which shows that the pore diameter of the cement paste specimens gradually decreased with age. Note that the pore structure curves of NC-0.3 and NG-0.03 were slightly offset to the bottom left compared to that of N-0, which indicates that NC and NG could improve the pore structure to make the microstructure more compact between 1 and 28 days. Therefore, the porosities of NC-0.3 and NG-0.03 at 28 days dropped by a large margin compared to that at 1 day. Moreover, the pore structure curve of NG-0.03 was at the bottom, and the porosity of NG-0.03 was the lowest, indicating that NG had the best effect in modifying the pore structure in the late stages.

3.6 SEM

SEM images of the cement paste with and without nanomaterials at 1 day are shown in Figure 10. The SEM image of N-0 at 1 day shows that only a small amount of acicular ettringite was formed, and there were many cracks and voids in the microstructure. More CH was embedded in the cement matrix of NC-0.3 after stacking, making the microstructure much denser at 1 day. On one hand, this confirmed the results obtained from MIP and XRD quantitative analyses. On the other hand, NC was regarded as a modifier that increased the order in the arrangement of CH. More flower-like ettringite, which was relatively dense, was generated in the cement paste with 0.03% NG. This is beneficial for improving the early compressive strength of the cement paste specimens. However, there were still more pores in the cement matrix of NG-0.03, consistent with the MIP results. Bykkam *et al.* [40] reported that some NG layers form interlinked three-dimensional sheets that generate a porous structure resembling a sponge, as shown in Figure 11. A large amount of reticulated ettringite and CH were formed in the cement paste containing NS, associated with the improvement in the early compressive strength of the cement paste. There were numerous nanopores in the ettringite, with a network structure, which also verified the deduction from the MIP analysis that NS could promote the generation of more nanopores with sizes of 0–30 nm at 1 day.

SEM images of the cement paste with and without nanomaterials at 28 days are shown in Figure 12. The cement paste containing NC generated less CH and C–S–H gel at 28 days than the N-0 cement paste, which led to a lower compressive strength gain for the former compared with the latter. In contrast, a large amount of C–S–H gel was formed in the NG-0.03 cement paste specimens, and CH was arranged in the cement matrix in an orderly manner, which made the microstructure much denser, thereby effectively improving the later compressive strength of the cement paste specimens. Although CH was inserted into the cement matrix of the NS-6 specimens in an orderly manner, there were still many cracks and nanopores in the cement matrix, resulting in low late compressive strength.

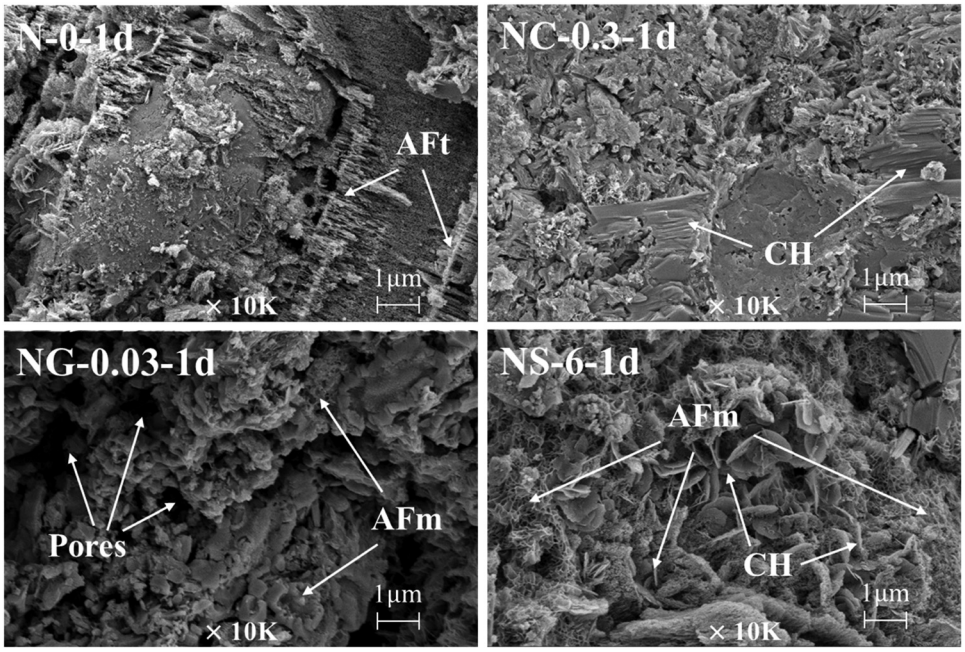

Figure 10: SEM images of the specimens with or without nanomaterials at 1 day.

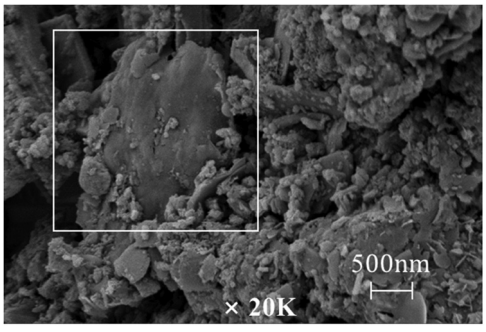

Figure 11: Layer-like structure of graphene oxide sheet.

3.7 Mechanisms for improving mechanical properties and microstructure of cement paste modified by different types of nanomaterials

Different types of nanomaterials modify cement paste *via* different mechanisms. The hydration models of cement with or without incorporated nanomaterials are shown in Figure 13, and the hydration reactions in the presence of the nanomaterials are shown in Figure 14. The nanoparticles can adhere to the surface of the cement particles to promote the formation of C–S–H seeds at an early age, after which the C–S–H seeds would be gradually transformed into C–S–H gel in the later stages. The detailed discussion is as follows.

Although the consumption of C_3S and C_2S in NC-0.3 was not the highest, the specimens of NC-0.3 showed the highest compressive strength at 1 day. This is because NC could accelerate the hydration process and react with C_3S, C_3A, and C_4AF to form C–S–H gel and carboaluminates (C–A–S–H gel) due to the increase in the Ca^{2+} concentration in the liquid phase [41,42]. As illustrated in Figure 10, CH was arranged in an orderly fashion between the cement particles, which made the cement matrix more compact. However, the denser matrix caused by the incorporation of NC at early ages could not provide available space for the formation of hydration products in the later stages [42], which resulted in the relatively low compressive strength of the specimens at 28 days.

The NG-0.03 mix at 1 day had a coarser structure than that of the other mixes. In fact, the addition of NG led to an increase in the proportion of capillary pores in the range of 100–1,000 nm, as shown in Figure 14b. Some NG layers form interlinked three-dimensional sheets that generate a porous structure resembling a sponge. Based on SEM observation, NG nanosheets can act as a template for cement hydration and regulate the formation of flower-like crystals [43–46], as shown in Figure 10. The main chemical components of the flower-like crystals might be ettringite, as deduced from the XRD results presented in Figure 5.

A possible hydration reaction in the presence of NS is shown in Figure 14c [47,48]. Because of the consumption

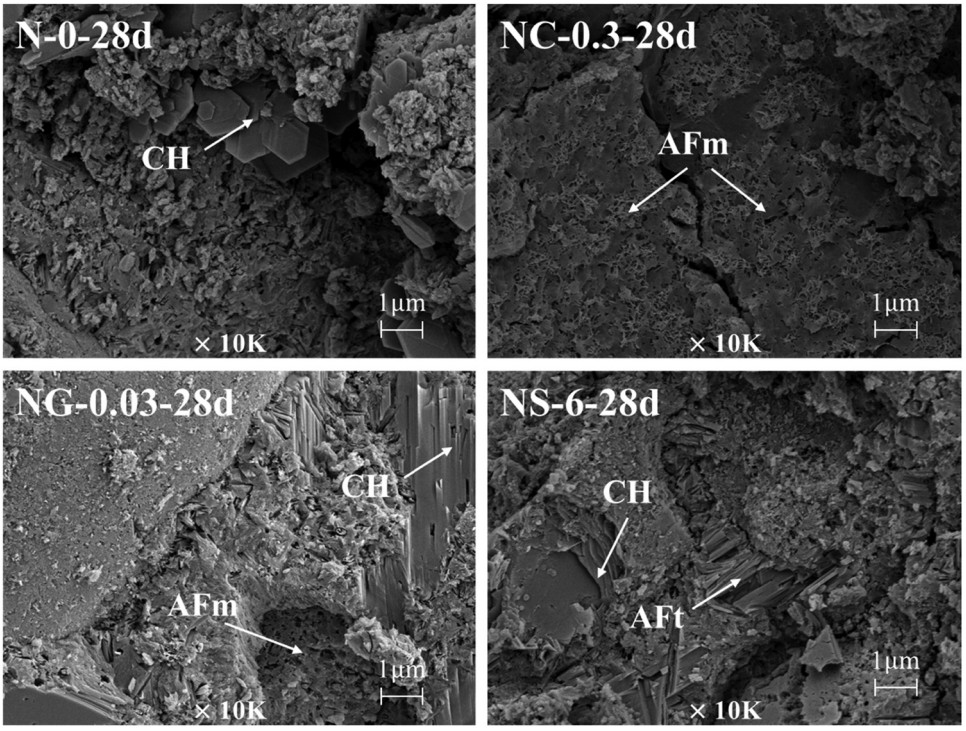

Figure 12: SEM images of the specimens with or without nanomaterials at 28 days.

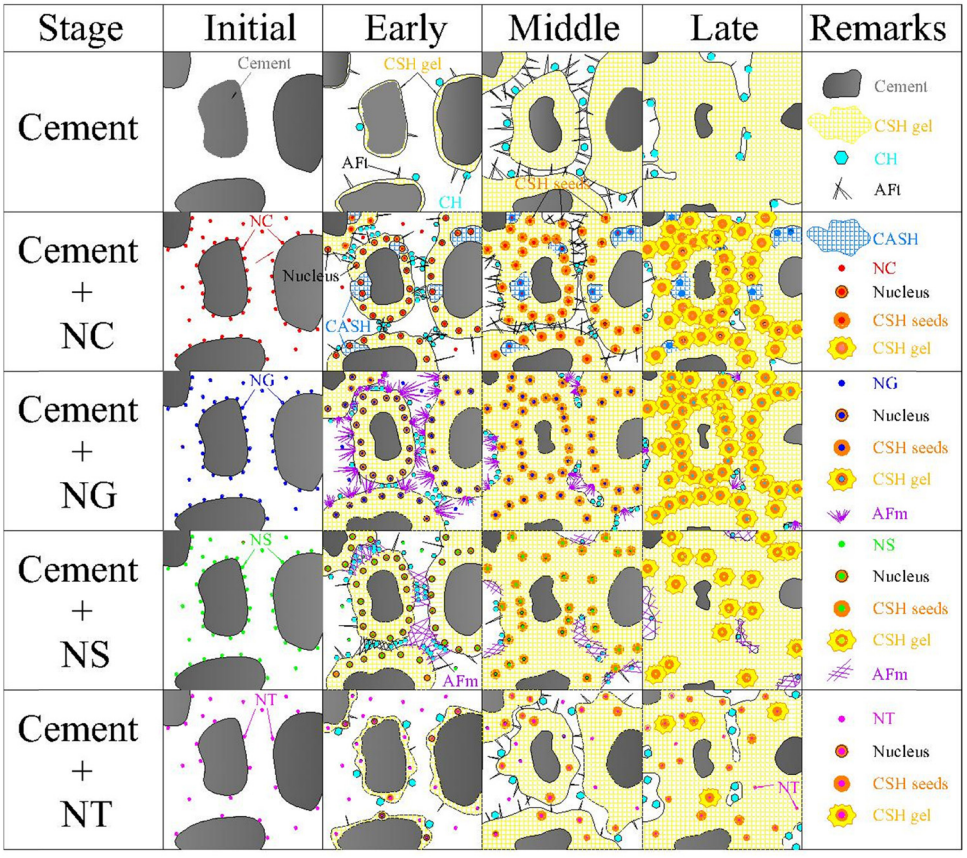

Figure 13: Hydration models of cement with or without incorporated nanomaterials.

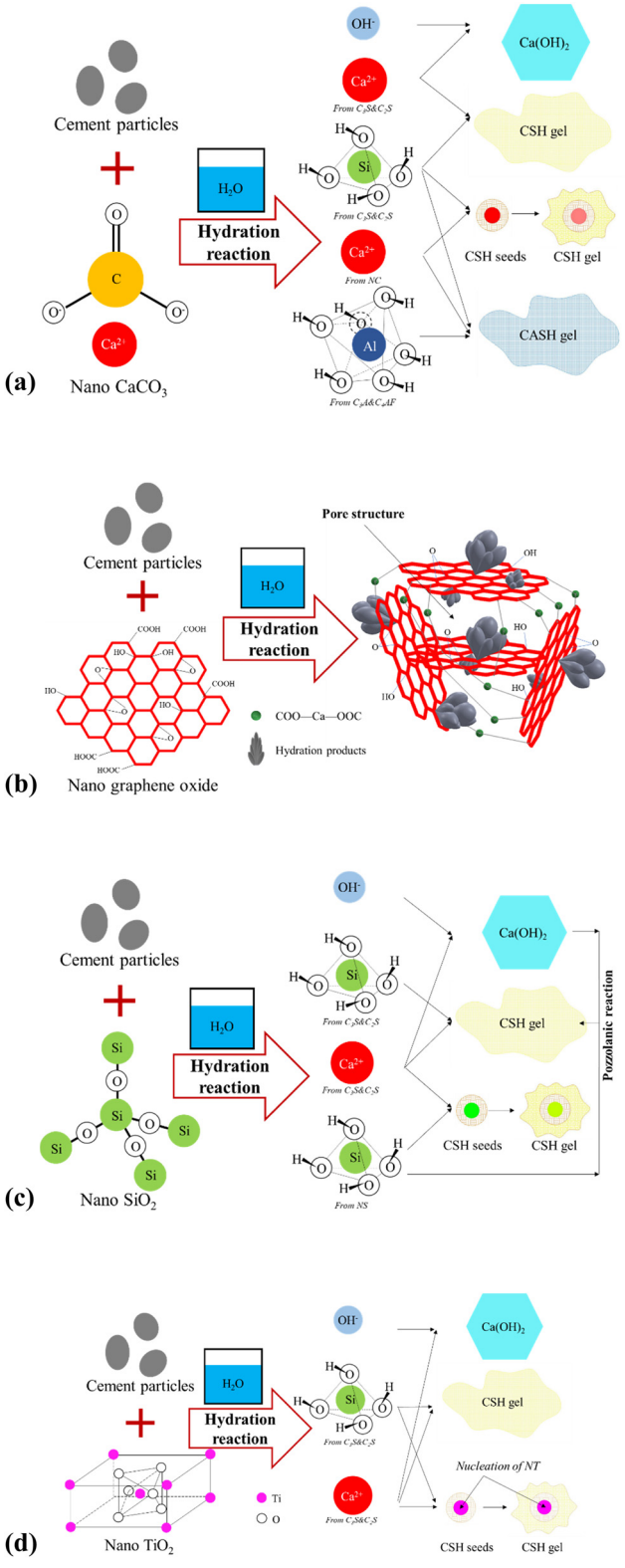

Figure 14: Hydration reactions in the presence of NC, NG, NS, and NT. (a) Hydration reactions in the presence of NC. (b) Hydration reactions in the presence of NG. (c) Hydration reactions in the presence of NS. (d) Hydration reactions in the presence of NT.

of Ca^{2+} by NS and the formation of C–S–H seeds, which accelerate the hydration process through seeding, C_3S and C_2S are constantly consumed and form more C–S–H gel and CH. This may be the reason why the hydration degree of NS-6 was the highest at 1 day. Moreover, the hydration product CH can undergo a pozzolanic reaction with additional NS, thereby decreasing the CH content in the later stages. Singh *et al.* [49] found that the addition of NS reduced the porosity of C–S–H, while increasing the gel porosity compared to the control cement paste, which was also reflected herein in the MIP results (Figure 9). Adding NS to cement can reduce the detrimental pores, despite the increase in less harmful and innocuous pores, which may account for the formation of a large amount of ettringite with a network structure between the cement particles, as shown in Figures 12 and 14.

NT could accelerate the cement hydration rate to some extent, but it was more inert in the cement hydration process compared with the other nanomaterials [50], which is reflected in the relatively lower consumption of C_3S and C_2S and the production of hydration products at 1 and 28 days. This may explain why the nucleation effect of NT was insignificant. Keivan *et al.* [51] reported that NT could retard the hydration of C_2S, thereby resulting in a decrease in the compressive strength of the cement paste at 28 days. The inclusion of NT could also depress the precipitation of CH [52], which might lead to an increase in the porosity at 1 day. In addition, CH could gradually precipitate in the cement matrix during the hydration process, and an appropriate loading of NT could increase the density of the cement paste at 28 days owing to its filling and seeding effect.

4 Conclusion

This study unveiled the strengthening mechanism of four different types of nanomaterials (NC, NG, NS, and NT) by comparing their effects on the mechanical properties and microstructure of cement paste. The key findings are summarised as follows:

(1) Appropriate incorporation of nanomaterials can improve the compressive strength of cement paste specimens at early ages due to more consumption of cement clinker and formation of hydration products but is not conducive to late strength development. For example, the compressive strength of the cement paste specimens with 0.3% NC was 27.1, 20.2, and 25.8% higher than that of N-0 at 1, 3, and 7 days,

respectively, but 10.4% lower than that of N-0 at 28 days.

(2) NC can react with cement clinker and modify the microstructure of cement paste. It could accelerate the hydration process and react with C_3S, C_3A, and C_4AF to form C–S–H gel and C–A–S–H gel due to the introduction of Ca^{2+}, which resulted in the improvement of compressive strength in the early stage. NC was also regarded as a modifier for increasing the order of the CH arrangement, leading to a more compact cement matrix.

(3) NG can act as a template for cement hydration and regulate the formation of hydration products. Although NG had little effect on the pore structure at 1 day due to the formation of a sponge-like structure due to the NG nanosheets, it could modify the microstructure and reduce the porosity of the specimen at later ages by promoting the formation of flower-like ettringite.

(4) NS can have hydration reaction with cement clinker and hydration product. $H_2SiO_4^{2-}$ formed by incorporating NS could not only react with Ca^{2+}, generating C–S–H seeds, but also have secondary hydration reaction with $Ca(OH)_2$, forming C–S–H gel, which would greatly improve the hydration of cement.

(5) NT exhibits insignificant nucleation effect and has inhibitory effect on portlandite precipitation. Exactly, NT is relatively inert in the cement hydration process, so only some NT plays a role of nucleation in the hydration of cement paste. Meanwhile, the inclusion of NT could also delay the precipitation of CH, which led to lower CH content in the early stage and higher in the later stages.

(6) Novel diagrams of hydration models and possible hydration reactions of cement in the presence of nanomaterials were drawn to compare and analyse the different modification mechanisms of different nanomaterials.

Further research is required to investigate the performance of different types of nanomaterials in cement-based material systems, such as mortar and concrete, as well as their long-term strength and durability performance. Moreover, the weak interface transition zone significantly restricts the strength and durability of cement-based materials. Therefore, it is necessary to explore the effects of different types of nanomaterials on the interface transition zone of cement-based materials.

Funding information: The authors are thankful for the financial support from the National Natural Science Foundation of China (52078453).

Author contributions: All authors have accepted responsibility for the entire content of this manuscript and approved its submission.

Conflict of interest: The authors state no conflict of interest.

References

[1] Nazar S, Yang J, Thomas BS, Azim I, Rehman SKU. Rheological properties of cementitious composites with and without nanomaterials: a comprehensive review. J Clean Prod. 2020;272:122701. doi: 10.1016/j.clepro.2020.122701.

[2] Zhao ZF, Qi TQ, Zhou W, Hui D, Xiao C, Qi JY, et al. A review on the properties, reinforcing effects, and commercialization of nanomaterials for cement-based materials. Nanotechnol Rev. 2020;9:303–22. doi: 10.1515/ntrev-2020-0023.

[3] Wu Q, Miao WS, Zhang YD, Gao HJ, Hui D. Mechanical properties of nanomaterials: a review. Nanotechnol Rev. 2020;9:259–73. doi: 10.1515/ntrev-2020-0021.

[4] Ren ZC, Liu YY, Yuan LW, Luan CQ, Wang JB, Cheng X, et al. Optimizing the content of nano-SiO_2, nano-TiO_2 and nano-$CaCO_3$ in Portland cement paste by response surface methodology. J Build Eng. 2021;35:102073. doi: 10.1016/j.jobe.2020.102073.

[5] Mohammad K, Hesam M. An investigation on the influence of nano silica morphology on the characteristics of cement composites. J Build Eng. 2020;30:101293. doi: 10.1016/j.jobe.2020.101293.

[6] Ahmed M, Serwan R, Wael M, Riyadh N, Hind A, Kawan G, et al. Microstructure characterizations, thermal properties, yield stress, plastic viscosity and compression strength of cement paste modified with nanosilica. J Mater Res Technol. 2020;9(5):10941–56. doi: 10.1016/j.jmrt.2020.07.083.

[7] Shuai B, Xinchun G, Guoyu L. Effect of the early-age frost damage and nano-SiO_2 modification on the properties of Portland cement paste. Constr Build Mater. 2020;262:120098. doi: 10.1016/j.conbuildmat.2020.120098.

[8] Ahmed M, Serwan R, Wael M, Riyadh N, Kawan G, Warzer Q, et al. Characterization and modeling the flow behavior and compression strength of the cement paste modified with silica nano-size at different temperature conditions. Constr Build Mater. 2020;257:119590. doi: 10.1016/j.conbuildmat.2020.119590.

[9] Lavergne F, Belhadi R, Carriat J, Ben Fraj A. Effect of nano-silica particles on the hydration, the rheology and the strength development of a blended cement paste. Cem Concr Compos. 2019;95:42–55. doi: 10.1016/j.cemconcomp.2018.10.007.

[10] Akin A. Investigation of different permeability properties of self-healing cementitious composites under colloidal nano silica curing conditions. Struct Concr. 2021. doi: 10.1002/suco.202000468.

[11] Lang L, Liu N, Chen B. Strength development of solidified dredged sludge containing humic acid with cement, lime and nano-SiO_2. Constr Build Mater. 2020;230:116971. doi: 10.1016/j.conbuildmat.2019.116971.

[12] Zhou F, Sun WB, Shao JL, Kong LJ, Geng XY. Experimental study on nano silica modified cement base grouting reinforcement materials. Geomech Eng. 2020;20:67–73. doi: 10.12989/gae.2020.20.1.067.
[13] Pengkun H, Shiho K, Deyu K, David JC, Jueshi Q, Surendra PS. Modification effects of colloidal nanoSiO_2 on cement hydration and its gel property. Compos B Eng. 2013;45:440–8. doi: 10.1016/j.compositesb.2012.05.056.
[14] Snehal K, Das BB, Akanksha M. Early age, hydration, mechanical and microstructure properties of nano-silica blended cementitious composites. Constr Build Mater. 2020;233:117212. doi: 10.1016/j.conbuildmat.2019.117212.
[15] Xiaohai L, Baoguo M, Hongbo T, Ting Z, Junpeng M, Huahui Q, et al. Effects of colloidal nano-SiO_2 on the immobilization of chloride ions in cement-fly ash system. Cem Concr Compos. 2020;110:103596. doi: 10.1016/j.cemconcomp.2020.103596.
[16] Deyu K, Haiwen P, Linhai W, David JC, Yang Y, Surendra PS, et al. Effect and mechanism of colloidal silica sol on properties and microstructure of the hardened cement-based materials as compared to nano-silica powder with agglomerates in micron-scale. Cem Concr Compos. 2019;98:137–49. doi: 10.1016/j.cemconcomp.2019.02.015.
[17] Haibin Y, Manuel M, Dapeng Z, Hongzhi C, Waiching T, Xiaohua B, et al. Effects of nano silica on the properties of cement-based materials: a comprehensive review. Constr Build Mater. 2021;282:122715. doi: 10.1016/j.conbuildmat.2021.122715.
[18] Mingli C, Xing M, Kaiyu H, Li L, Shirley S. Effect of macro-, micro- and nano-calcium carbonate on properties of cementitious composites – a review. Materials. 2019;12:781. doi: 10.3390/ma12050781.
[19] Teixeira CS, Wasielewsky JC, dos Santos GS, Bernardi A, Bortoluzzi EA, Roberti Garcia LF. Effect of the addition of nanoparticles of $CaCO_3$ and different water-to-powder ratios on the physicochemical properties of white Portland cement. Microsc Res Tech. 2021;84:592–601. doi: 10.1002/jemt.23617.
[20] Taijiro S, Fatoumata D. Seeding effect of Nano-$CaCO_3$ on the hydration of tricalcium silicate. Transport Res Res. 2010;2141:61–7. doi: 10.3141/2141-11.
[21] Yang HS, Li WW, Che YJ. 3D printing cementitious materials containing nano-$CaCO_3$: workability, strength, and microstructure. Front Mater. 2020;7:260. doi: 10.3389/fmats.2020.00260.
[22] Anwar H, Faiz UAS. Influence of nano-$CaCO_3$ addition on the compressive strength and microstructure of high volume slag and high volume slag-fly ash blended pastes. J Build Eng. 2020;27:100929. doi: 10.1016/j.jobe.2019.100929.
[23] Zhang S, Qiao WG, Wu Y, Fan ZW, Zhang L. Optimization of microfine-cement-based slurry containing microfine fly ash and nano-$CaCO_3$ for microfracture grouting. B Eng Geol Environ. 2021;80. doi: 10.1007/s10064-021-02199-1.
[24] Faiz UAS, Steve WMS. Chloride induced corrosion durability of high volume fly ash concretes containing nano particles. Constr Build Mater. 2015;99:208–25. doi: 10.1016/j.conbuildmat.2015.09.030.
[25] Shiho K, Pengkun H, David JC, Surendra PS. Modification of cement-based materials with nanoparticles. Cem Concr Compos. 2013;36:8–15. doi: 10.1016/j.cemconcomp.2012.06.012.
[26] Zhen L, Siqi D, Xun Y, Baoguo H, Jinping O. Multifunctional cementitious composites modified with nano titanium dioxide: a review. Compos Part A. 2018;111:115–37. doi: 10.1016/j.compositesa.2018.05.019.
[27] Ikotun BD, Raheem AA. Characteristics of Wood Ash Cement Mortar Incorporating Green-Synthesized Nano-TiO_2. Int J Concr Struct M. 2021;15. doi: 10.1186/s40069-021-00456-x.
[28] Wang J, Xu YQ, Wu XP, Zhang P, Hu SW. Advances of graphene- and graphene oxide-modified cementitious materials. Nanotechnol Rev. 2020;9:465–77. doi: 10.1515/ntrev-2020-0041.
[29] Lingchao L, Piqi Z, Zeyu L. A short discussion on how to effectively use graphene oxide to reinforce cementitious composites. Constr Build Mater. 2018;189:33–41. doi: 10.1016/j.conbuildmat.2018.08.170.
[30] Karthik C, Rama MRP. An intense review on the performance of graphene oxide and reduced graphene oxide in an admixed cement system. Constr Build Mater. 2020;259:120598. doi: 10.1016/j.conbuildmat.2020.120598.
[31] Li Z, Xinli G, Luguang S, Yang S, Guozhong D, Jiaping L. An intensive review on the role of graphene oxide in cement-based materials. Constr Build Mater. 2020;241:117939. doi: 10.1016/j.conbuildmat.2019.117939.
[32] Weijin L, Guoxue Z. Effect of reduced graphene oxide on the early-age mechanical properties of geopolymer cement. Mater Lett. 2020;276:128223. doi: 10.1016/j.matlet.2020.128223.
[33] Mokhtar MM, Abo-El-Enein SA, Hassaan MY, Morsy MS, Khalil MH. Mechanical performance, pore structure and micro-structural characteristics of graphene oxide nano platelets reinforced cement. Constr Build Mater. 2017;138:333–9. doi: 10.1016/j.conbuildmat.2017.02.021.
[34] Karthik C, Rama MRP. Strength properties of graphene oxide cement composites. Mater Today. 2020;8:1–5. doi: 10.1016/j.matpr.2020.08.369.
[35] Devi SC, Khan RA. Effect of graphene oxide on mechanical and durability performance of concrete. J Build Eng. 2020;27:101007. doi: 10.1016/j.jobe.2019.101007.
[36] Liu YT, Chen B, Qin ZH. Effect of nano-silica on properties and microstructures of magnesium phosphate cement. Constr Build Mater. 2020;264:120728. doi: 10.1016/j.conbuildmat.2020.120728.
[37] Bhatty JI. Hydration versus strength in a Portland cement developed from domestic mineral wastes – a comparative study. Thermochim Acta. 1986;106:93–103.
[38] El-Jazairi B, Illston JM. The hydration of cement paste using the semi-isothermal method of derivative thermogravimetry. Cem Concr Compos. 1980;10:361–6.
[39] Monteagudo SM, Moragues A, Gálvez JC, Casati MJ, Reyes E. The degree of hydration assessment of blended cement pastes by differential thermal and thermogravimetric analysis. Morphological evolution of the solid phases. Thermochim Acta. 2014;592:37–51.
[40] Bykkam S, Rao KV, Chakra CHS, Thunugunta T. Synthesis and characterization of graphene oxide and its antimicrobial activity against *Klebseilla* and *Staphylococcus*. Int J Adv Biotechnol Res. 2013;4:142–6.
[41] Makar JM, Chan GW, Beaudoin JJ, Torres F, Trischuk K. Effect of n-$CaCO_3$ and metakaolin on hydrated Portland cement. Adv Cem Res. 2012;24:211–9. doi: 10.1680/adcr.11.00010.

[42] Wu Z, Shi C, Khayat KH, Wan S. Effects of different nanomaterials on hardening and performance of ultra-high strength concrete (UHSC). Cem Concr Compos. 2016;70:24–34. doi: 10.1016/j.cemconcomp.2016.03.003.
[43] Shenghua L, Jingjing L, Ting S, Yujuan M, Qingfang Z. Effect of GO nanosheets on shapes of cement hydration crystals and their formation process. Constr Build Mater. 2014;64:231–9. doi: 10.1016/j.conbuildmat.2014.04.061.
[44] Shenghua L, Yujuan M, Chaochao Q, Ting S, Jingjing L, Qingfang Z. Effect of graphene oxide nanosheets of microstructure and mechanical properties of cement composites. Constr Build Mater. 2013;49:121–7. doi: 10.1016/j.conbuildmat.2013.08.022.
[45] Shenghua L, Sun T, Jingjing L, Qingfang Z. Use of graphene oxide nanosheets to regulate the microstructure of hardened cement paste to increase its strength and toughness. CrystEngComm. 2014;16:8508–16. doi: 10.1039/c4ce00684d.
[46] Lv SH, Ma YJ, Qiu CC, Zhou QF. Regulation of GO on cement hydration crystals and its toughening effect. Mag Concrete Res. 2013;65:1246–54. doi: 10.1680/macr.13.00190.
[47] Singh LP, Bhattacharyya SK, Shah SP, Mishra G, Ahalawat S, Sharma U. Studies on early stage hydration of tricalcium silicate incorporating silica nanoparticles: Part I. Constr Build Mater. 2015;74:278–86. doi: 10.1016/j.conbuildmat.2014.08.046.
[48] Singh LP, Bhattacharyya SK, Shah SP, Mishra G, Sharma U. Studies on early stage hydration of tricalcium silicate incorporating silica nanoparticles: Part II. Constr Build Mater. 2016;102:943–9. doi: 10.1016/j.conbuildmat.2015.05.084.
[49] Singh LP, Ali D, Sharma U. Studies on optimization of silica nanoparticles dosage in cementitious system. Cem Concr Compos. 2016;70:60–8. doi: 10.1016/j.cemconcomp.2016.03.006.
[50] Jun C, Shi-cong K, Chi-sun P. Hydration and properties of nano-TiO_2 blended cement composites. Cem Concr Compos. 2012;34:642–9. doi: 10.1016/j.cemconcomp.2012.02.009.
[51] Keivan A, Keivan A, Behfarnia K. The effects of TiO_2 and ZnO nanoparticles on physical and mechanical properties of normal concrete. Asian J Civ Eng. 2013;14:517–31.
[52] Kurihara R, Maruyama I. Influences of nano-TiO_2 particles on alteration of microstructure of hardened cement. https://www.researchgate.net/publication/304755102